

**MOL #41152**

PD-307243 Causes Instantaneous Current through Human *Ether-a-go-go*-Related  
Gene (hERG) Potassium Channels

Earl Gordon, Irina M. Lozinskaya, Zuojun Lin, Simon F. Semus, Frank E. Blaney,  
Robert N. Willette, Xiaoping Xu

Cardiovascular and Urogenital Center of Excellence in Drug Discovery and Department  
of Computational and Structural Sciences, GlaxoSmithKline, King of Prussia, PA 19406,  
USA (E.G., I.M.L., Z.L., S.F.S., R.N.W, X.X.); and Department of Computational and  
Structural Sciences, GlaxoSmithKline, New Frontiers Science Park, Third Avenue,  
Harlow, Essex CM19 5AW, UK (F.E.B.)

a) Running Title: hERG channel activator PD-307243

b) Correspondence Author: Xiaoping Xu, GlaxoSmithKline, 709 Swedeland Road,  
UW2511, PO Box 1539, King of Prussia, PA 19406, USA

Telephone: (610) 270-6858

Fax: (610) 270-6206

E-mail: Xiaoping.2.Xu@gsk.com

c) Number of Text pages: 35

Number of Tables: 0

Number of Figures: 11

Number of References: 33

Number of words in the Abstract: 244

Number of words in the Introduction: 536

Number of words in the Discussion: 1310

d) Abbreviations: CHO, Chinese hamster ovary; hERG, human ether-a-go-go-related gene; I, instantaneous current;  $I_{Kr}$ , rapid component of delayed rectifier  $K^+$  current;  $I_{to}$ , transient outward  $K^+$  current; I-V, current-voltage relationship; LQTS, long QT syndromes; SQTs, short QT syndromes; S, step current; T, tail current

**Abstract**

Long and short QT syndromes associated with loss and gain of hERG channel activity, respectively, can cause life threatening arrhythmias. As such, modulation of hERG channel activity is an important consideration in the development of all new therapeutic agents. In the present study we investigated the mechanisms of action of PD-307243, a known hERG channel activator, on hERG channels stably expressed in CHO cells using the patch-clamp technique. In the whole-cell recordings, the extracellular application of PD-307243 concentration-dependently increased the hERG current and markedly slowed hERG channel deactivation and inactivation. PD-307243 had no effect on the selectivity filter of hERG channels. The activity of PD-307243 was use-dependent. PD-307243 (3 and 10  $\mu\text{M}$ ) induced instantaneous hERG current with little decay at membrane potentials from -120 to -40 mV. At more positive voltages, PD-307243 induced an  $I_{\text{to}}$ -like upstroke of hERG current. The actions of PD-307243 on the rapid component of delayed rectifier  $\text{K}^+$  current ( $I_{\text{Kr}}$ ) in rabbit ventricular myocytes were similar to those observed in hERG channel transfected CHO cells. Inside-out patch experiments revealed that PD-307243 increased hERG tail currents by  $2.1 \pm 0.6$  ( $n=7$ ) and  $3.4 \pm 0.3$  fold ( $n=4$ ) at 3 and 10  $\mu\text{M}$ , respectively, by slowing the channel deactivation but had no effect on channel activation. During a voltage-clamp protocol using a prerecorded cardiac action potential, 3  $\mu\text{M}$  PD-307243 increased the total potassium ions passed through hERG channels by  $8.8 \pm 1.0$  fold ( $n=5$ ). Docking studies suggest that PD-307243 interacts with residues in the S5-P region of the channel.

Ion channels may represent chemically tractable and biologically attractive targets, but they are just as likely to present off-target challenges that portend serious safety liabilities for new therapeutic agents. Thus, an understanding of ion channel selectivity and mechanism of action are important goals in the optimization of drug efficacy and safety. Particularly troublesome are activities at the hERG channel that normally passes the rapid component of the delayed rectifier K<sup>+</sup> current (I<sub>Kr</sub>) which plays a critical role in phase III repolarization of ventricular action potentials (Abbott *et al.*, 1999). In fact, it is now commonplace to screen compounds for their activity against hERG channels because it is known that inhibition of this channel is associated with the development of long QT syndrome (LQTS) (Brown, 2005; Wible *et al.*, 2005). LQTS can lead to the development of life threatening arrhythmias; this is clearly an unwanted effect in particular for non-cardiac drugs.

Until recently (Brugada *et al.*, 2004), there was a paucity of information on the link between the hERG channel and the development of short QT syndrome (SQTS). However, it is now known that some instances of SQTS are linked to gain-of-function mutations in hERG channels (Brugada *et al.*, 2004). We can also speculate that certain small molecules that are activators of hERG channels could result in modification of the QT interval and lead to the development of SQTS. On the other hand, hERG channel activators might also be of therapeutic usage in individuals with conditions of delayed repolarization, LQTS being the most notable example (Seeböhm, 2005). LQTS is a condition that has been shown to be underlined by mutations in a number of ion channel genes, for example, hERG, KCNQ1 and Na<sub>v</sub>1.5 among others, and also by mutations in

## MOL #41152

channel related genes, such as members of the KNCE family (Modell and Lehmann, 2006). Having detailed knowledge of the mechanisms by which these compounds activate the hERG channel will therefore provide a useful starting point for the development of lead compounds that could potentially be useful in the treatment of such conditions.

At present only five hERG activators have been studied in great detail: RPR260243 (Kang *et al.*, 2005), NS1643 (Casis *et al.*, 2006; Hansen *et al.*, 2006a), NS3623 (Hansen *et al.*, 2006b), PD-118057 (Zhou *et al.*, 2005) and Mallotoxin (Zeng *et al.*, 2006). PD-307243 is a member of a series of compounds that have previously been reported to be activators of hERG channels (Zhou *et al.*, 2005). The previous report is centered on the effects of PD-118057 which causes shortening of the action potential duration and QT-interval and prevents early after-depolarizations caused by Dofetilide in arterially perfused rabbit ventricular wedge preparation (Seeböhm, 2005; Zhou *et al.*, 2005). PD-307243 has been shown to increase hERG tail current by 58% at 1  $\mu$ M, this is more potent than PD-118057 (Zhou *et al.*, 2005). However, the concentration-dependent effects and the possible mechanisms by which this activation occurs have not been characterized. Herein, we report the putative mechanisms of action of PD-307243 on hERG channels expressed in CHO cells. We found that this drug increased hERG current mainly by slowing hERG channel deactivation and inactivation. Additionally we also demonstrated the activating effects of PD-307243 on  $I_{Kr}$  of rabbit ventricular myocytes.

## **Materials and Methods**

### Cell culture

Chinese hamster ovary (CHO) cells were stably transfected to express hERG channels (BioCat ID: 97761, GlaxoSmithKline) and used for patch-clamp recording. The reason we chose CHO cells to stably express hERG channels is that CHO cells have little endogenous voltage-dependent potassium channels and therefore are widely used to express voltage-gated potassium channels (Zeng *et al.*, 2005). CHO cells expressing hERG channels were maintained at 37°C with 5% CO<sub>2</sub> in six-well culture dishes with Iscoves DMEM F-12 nutrient mixture, supplemented with 10% FBS, 100 U/ml penicillin and streptomycin, and 0.5 mg/ml geneticin (Invitrogen, Carlsbad, CA).

### Single ventricular myocyte isolation

The studies were carried out in accordance with the Guide for the Care and Use of Laboratory Animals as adopted and promulgated by the U.S. National Institutes of Health and approved by the GlaxoSmithKline Animal Care and Use Committee. Cardiac myocytes were isolated from the right ventricle of adult male New Zealand White rabbits using enzyme digestion described previously (Rials *et al.*, 1997).

### Patch-clamp

Whole-cell and inside-out patch currents were recorded from CHO cells stably expressing hERG channels and freshly isolated rabbit ventricular myocytes with an Axopatch 200B amplifier and Digidata 1322A digitizer (Molecular Devices, Union City, CA). Glass electrodes (2-4 M $\Omega$  resistance) were pulled from thin wall glass (WPI,

## MOL #41152

Sarasota, FL) using a P-97 horizontal puller (Sutter, Novato, CA) and fire polished with MF-830 micro forge (Narishige, Long Island, NY). Cells were placed in a small chamber (volume=0.7 ml) and continuously perfused with an external solution (3-4 ml/min). In whole-cell recording of CHO cells, bath solution contained (in mM) 140 NaCl, 4 KCl, 1 MgCl<sub>2</sub>, 2 CaCl<sub>2</sub>, 10 Glucose, and 10 HEPES, pH=7.4. In the case of ventricular myocytes, bath solution contained (in mM) 132 NMDG-Cl, 5 KCl, 1.2 MgCl<sub>2</sub>, 10 Glucose, 10 HEPES, 0.1 BaCl<sub>2</sub>, pH=7.4. Nifedipine (1 μM) was added to block L-type Ca<sup>2+</sup> current. Pipette solution contained (in mM) 119 K-gluconate, 15 KCl, 5 EGTA, 5 K<sub>2</sub>ATP, 3.2 MgCl<sub>2</sub>, 5 HEPES, pH=7.2. In inside-out patch recording, both bath and pipette solution contained (in mM) 140 KCl, 1 MgCl<sub>2</sub>, 2 CaCl<sub>2</sub>, 5 HEPES, pH=7.2. Currents were elicited by different voltage protocols (described in text and figure legends) and acquired with pCLAMP 8 software (Molecular Devices, Union City, CA) at room temperature. Whole-cell capacity transient was compensated near completely. Only cells with GΩ seal were used for hERG current and I<sub>Kr</sub> recording. No leak correction was applied.

### Chemicals

PD-307243 (prepared by the chemists at GlaxoSmithKline, chemical structure shown in the inset of Fig. 1B), nifedipine (MP Biomedicals, Solon, OH) and Dofetilide (APIN chemicals LTD, Abingdon, UK) were made as 10 mM dimethyl sulfoxide stock solutions and diluted in the bath solutions to desired concentrations.

## Molecular Modeling

The initial hERG channel model was based upon the rat open state Kv1.2 crystal structure (Long *et al.*, 2005) and has been previously described (Micheli *et al.*, 2007). The loop region between the S5 and pore helices was then subsequently modified to ensure consistency with the biophysical data and molecular model recently published (Tseng *et al.*, 2007). The S5-P linker was modeled using the software package MOE with the two predicted alpha-helical domains, H576-I583 and W585-G594, constructed with the default parameters employed in the program. The modified linker was then inserted between the S5 and pore helices by appropriate manual adjustment of the backbone torsion angles to ensure optimal alignment of the terminal residues. The process was repeated for the remaining three repeat domains and the resulting structure was geometry optimized using the OPLS 2005 force field as implemented in MacroModel (Schrodinger LLC., New York, NY). Molecular docking of the hERG channel activator, PD-370243, was performed with Glide (Schrodinger LLC. New York, NY) using the default SP parameters.

## Data analysis

All data were analyzed and illustrated using pCLAMP 8, Origin 7 (OriginLab Corp., Northampton, MA) and Excel (Microsoft) and presented as mean±S.E. (n). Zero current level was indicated using dashed lines in all figures. Statistic significance ( $p < 0.05$ ) was determined using one way ANOVA or paired t-test.



## Results

### PD-307243 activates hERG channel

When hERG currents were induced with a 2-s pulse to +20 mV followed by a 2-s tail step at -50 mV delivered every 10-s (Fig. 1 A, inset), bath perfusion of PD-307243 (10  $\mu$ M) resulted in a gradual increase in both step and tail currents (Fig. 1A). Surprisingly, continuous perfusion with 10  $\mu$ M PD-307243 and constant stimulus resulted in an  $I_{to}$ -like current which is highlighted in Fig. 1A, upper panel. Compared with the tail peak current, the onset of this  $I_{to}$ -like current was slower and took a much longer time to reach steady-state (Fig. 1A, lower panel). Interestingly, the activation of the  $I_{to}$ -like current is seemingly dependent on channel opening. Continuous perfusion with 10  $\mu$ M PD-307243 in the absence of stimulating pulses for four and a half minutes did not result in the generation of the  $I_{to}$ -like current at the 1<sup>st</sup> stimulus pulse (Fig. 1B, upper panel, trace labeled as 1<sup>st</sup>), whereas increases in both step and tail currents were observed.

The activating effects of PD-307243 on hERG channels at various depolarization voltages were further investigated by a voltage protocol shown in Fig. 2A (inset). After recording control hERG current traces (left panel), 10  $\mu$ M PD-307243 was perfused into the recording chamber and the cells were continuously stimulated with the pulse shown in Fig. 1A (inset) at 10-s intervals until the drug effect reached steady-state. The hERG current traces at various test potentials were recorded (middle panel, note the different current amplitude scale). The third group of hERG traces was recorded after extensive washout (~30 min) with control solution (right panel). The corresponding current-voltage

## MOL #41152

relationships (I-V) for the instantaneous current (I), the step current (S), and the tail peak current (T) are shown to highlight changes that can be attributed to the effects of the compound on hERG gating (Fig. 2B). From this initial set of experiments we observed that 10  $\mu$ M PD-307243 increased all three current amplitudes (I, S and T). It caused persistent hERG current at membrane potential as low as -60 mV. In addition, the hERG channel lost its characteristic rectification. The deactivation at -50 mV was extremely slow.

To further characterize the effects of the compound, we recorded step currents using an expanded voltage range (-100 mV to +80 mV) and measured the tail currents at -120 mV to allow more complete deactivation (Fig. 3A, inset). As illustrated in Fig. 3A, 3  $\mu$ M PD-307243 at steady-state induced instantaneous currents with little decay at very negative step voltages ( $\leq$  -40 mV). When the step voltages became more positive, an inactivating phase appeared (Fig. 3A [2]). Dofetilide (1  $\mu$ M), a specific blocker of hERG currents (Jurkiewicz and Sanguinetti, 1993), was able to completely block currents activated by 3  $\mu$ M PD-307243 (Fig. 3A [3]), confirming that the instantaneous current is through hERG channels and not due to the upregulation of other channels endogenous to CHO cells (Lalik *et al.*, 1993; Yu and Kerchner, 1998). The fact that PD-307243 (10  $\mu$ M) did not activate any current in untransfected CHO cells (n=3, data not shown) further validated this point. The decay of the tail current at -120 mV following +20 mV depolarization step was fitted with a two-exponential function to determine the deactivation time constants. There was a statistically significant slowing of both the fast and slow deactivation time constants,  $\tau_f$  was  $17 \pm 3$  ms and  $72 \pm 16$  ms (n=8),  $\tau_s$  was  $55 \pm 8$

ms and  $199 \pm 26$  ms ( $n = 8$ ) for the control and 3  $\mu\text{M}$  PD-307243 perfused cells, respectively.

The current voltage (I-V) relationship shown in Fig. 3B revealed the concentration-dependent effects of PD-307243. Under control condition, very little instantaneous current was detected. PD-307243 induced instantaneous current at voltage steps  $\geq +20$  mV with 1  $\mu\text{M}$ , and at all voltage steps with 3 and 10  $\mu\text{M}$  (left panel). Before drug treatment, the I-V relationship of hERG step current had characteristic rectification with the maximal step current being observed at +30 mV ( $578 \pm 144$  pA,  $n=8$ ). The maximal step current was increased and the voltage at which the maximum was reached shifted to +40 mV ( $1716 \pm 538$  pA,  $n=6$ ) and +60 mV ( $3180 \pm 676$  pA,  $n=8$ ) in the presence of 1 and 3  $\mu\text{M}$  PD-307243. No reduction of step current was seen up to +80 mV with a concentration of 10  $\mu\text{M}$  PD-307243 (middle panel). Under control conditions, no hERG tail current was recorded at step voltages  $\leq -40$  mV. PD-307243 (1  $\mu\text{M}$ ) slightly increased the tail current. Concentrations of 3 and 10  $\mu\text{M}$  PD-307243 induced large tail currents even at step voltages from -100 to -40 mV (right panel) and the reduction of tail peak current within this voltage range reflect the minor voltage-dependent hERG channel inactivation. The increase in tail peak currents at voltages  $\geq -30$  mV is due to the voltage-dependent activation of hERG channels.

The appearance of persistent hERG current at negative voltages in the presence of PD-307243 required the opening of the hERG channels. Using the same protocol from the previous experiment (Fig. 3A) but limiting the maximal pulse step to -40 mV to avoid

## MOL #41152

activating hERG channels, we assessed the effect of 6 minutes of PD-307243 (3  $\mu$ M) perfusion without stimulus and observed no current activation in the voltage range tested (Fig. 4A, middle vs. left). After stimulating the cell with the protocol shown in Fig. 1A (inset) for several minutes, we observed persistent hERG current at voltage steps from -100 mV to -40 mV (Fig. 4A, right). The corresponding I-Vs were shown in Fig. 4B.

In the presence of 3  $\mu$ M PD-307243, a large component of the hERG tail current remained at the end of 2-s step of -120 mV (Fig. 2A [2]). To investigate whether the hERG channels would eventually close, we increased the interval between depolarizing pulses to 2-min and decreased the membrane potential to -130 mV (Fig. 5A, top panel). After recording a control trace, the cell was perfused for two-min with 3  $\mu$ M PD-307243 and subsequent recordings were made with continuous perfusion of the compound. In the presence of PD-307243, there was incomplete deactivation even with the very long interval and very negative voltage between depolarizing pulses (Fig. 5A, middle panel). The  $I_{to}$ -like current was observed at the second pulse in the presence of the compound (Fig. 5A, bottom panel); highlighting that it is a use-dependent phenomenon.

To investigate if the compound had any effect on the hERG channel selectivity filter we depolarized the channels with a step to +40 mV for 2-s and then recorded tail currents in a range of voltages between -120 to -40 mV for 2-s (Fig 5B, inset). The reversal potential was not altered in the presence of 3  $\mu$ M PD-307243 (Fig. 5B), the average values were  $-79.5 \pm 1.0$  and  $-78.4 \pm 0.7$  mV ( $n=3$ ) for control and 3  $\mu$ M PD-307243

respectively ( $P > 0.05$ ). This result implies that PD-307243 does not disrupt the selectivity filter.

### **PD-307243 impairs hERG channel inactivation**

The removal of rectification of hERG step I-V shown earlier suggests that there is modification in hERG channel inactivation. We investigated the effect of PD-307243 (3  $\mu$ M) on channel inactivation by using a protocol that has been used (Zou *et al.*, 1998) to determine the voltage-dependence of recovery from inactivation (Fig. 6A, inset). After control current traces were recorded (Fig. 6A, left), the cells were perfused with 3  $\mu$ M PD-307243 and stimulated with the protocol shown in Fig. 1A (inset) until the drug effect reached steady-state, subsequently a second group of current traces was recorded (Fig. 6A, right). PD-307243 shifted the voltage-dependent recovery from inactivation of hERG channels; the difference was significant at membrane potentials  $\geq 0$  mV. Fitting the data using the Boltzmann equation found  $V_{1/2}$  to be -43 mV and -27 mV, and the slope factor ( $k$ ) was 23 mV and 39 mV for the control and the treated group, respectively (Fig. 6B).

We next examined the effect of 3  $\mu$ M PD-307243 on the onset rate of hERG current inactivation using a previously described three step protocol (Fig. 7A, inset) (Smith *et al.*, 1996; Spector *et al.*, 1996). The results indicated a significant slowing of the rate of channel inactivation; the inactivation time constant was obtained using a single exponential fit (Fig. 7B). As the membrane potential increased, while there was the

usual acceleration of inactivation in the control group, surprisingly, the drug group showed a significant slowing of inactivation.

### **PD-307243 acts on hERG channels in the inside-out patch configuration**

The results from the whole-cell experiments indicate that there is a significant slowing of inactivation as well as a slowing of the deactivation of hERG channels in the presence of PD-307243, giving rise to the possibility that the compound could have multiple sites of action. To test this hypothesis, recordings were made in the inside-out patch configuration using a voltage protocol (Fig. 8A inset) that was applied to the patch repeatedly at 10-s interval. Representative current traces in control, 3 and 10  $\mu\text{M}$  drug at steady-state and after prolonged washout were illustrated in Fig. 8A. We observed that there was an increase in tail current amplitude and slowing of deactivation in the presence of PD-307243 (3 and 10  $\mu\text{M}$ ). The peak tail was increased  $2.1 \pm 0.6$  fold ( $n=7$ ) and  $3.4 \pm 0.3$  fold ( $n=4$ ), respectively, in the presence of 3 and 10  $\mu\text{M}$  PD-307243. The fast deactivation time constant of the tail current ( $\tau_f$ ) was  $17 \pm 5$  ms and  $50 \pm 12$  ms ( $n=7$ ) for control and 3  $\mu\text{M}$  PD-307243, and the slow deactivation time constant ( $\tau_s$ ) was  $42 \pm 12$  ms in control compared to  $118 \pm 26$  ms ( $n=7$ ) obtained after perfusion with 3  $\mu\text{M}$  PD-307243 ( $P < 0.05$ ). The activation effect of PD-307243 could also be largely reversed by washout of the compound (Fig. 8A) or completely blocked by 1  $\mu\text{M}$  Dofetilide (data not shown).

We further examined how PD-307243 affected the voltage-dependent activation of hERG current in inside-out patches. The voltage protocol (Fig. 8B, inset) was identical

to what used in the whole-cell experiment (Fig. 3A inset). The major effect of PD-307243 was a concentration-dependent increase of the tail current amplitude and slowing of deactivation (Fig. 8B). All the tail currents were normalized by the amplitude of the control tail current following +80 mV depolarization and plotted against step membrane potentials for control, 3 and 10  $\mu$ M PD-307243 (Fig. 8C). The maximal tail current following the +80 mV step was increased 2.5- and 3.8-fold compared to control with concentrations of 3 and 10  $\mu$ M PD-307243, respectively. However, the half maximal activation voltage ( $V_{1/2}$ ) obtained by fitting the data with the Boltzmann equation was not changed:  $V_{1/2}$  was  $9.7 \pm 7.9$  mV ( $n=3$ ),  $13.5 \pm 1.7$  mV ( $n=3$ ) and  $10.7 \pm 2.5$  mV ( $n=2$ ) for control, 3 and 10  $\mu$ M PD-307243 ( $P > 0.05$ ). When applied on the intracellular side of the membrane, PD-307243 did not induce  $I_{to}$ -like hERG current at depolarizing voltage steps and only very small persistent current was seen at step voltages  $\leq -80$  mV in the presence of the drug (Fig. 8C).

### **PD-307243 activates $I_{Kr}$ in rabbit ventricular myocytes**

Next, we wanted to confirm the unique activation effects of PD-307243 on hERG channels expressed in CHO cells could be reproduced in native cells expressing the rapid component of delayed rectifier  $K^+$  ( $I_{Kr}$ ) channels. For this purpose we recorded currents from ventricular myocytes freshly isolated from the rabbit heart. Membrane current (Fig. 9A, left panel) was elicited by the voltage-clamp protocol shown in the inset when  $Na^+$ ,  $Ca^{2+}$  and inward rectifier  $K^+$  current were eliminated by ion substitution and blocking agents in the external solution. The cell was then perfused with 3  $\mu$ M PD-307243 and repeatedly stimulated by the same protocol until drug effects reached

steady-state. The second group of current traces were then recorded which clearly demonstrated the activation effects of PD-307243 (Fig. 9A, middle panel). The currents activated by PD-307243 at -30 mV, 0 mV and +30 mV were obtained by subtracting the control current traces from the corresponding recordings in the presence of the drug (Fig. 9A, right panel). The PD-307243 activated an  $I_{to}$ -like current, which resembles the drug effect observed in CHO cells expressing hERG channels. Similar results were obtained in two additional ventricular myocytes. We further confirmed that the PD-307243 activated current was  $I_{Kr}$  by demonstrating its inhibition by 1  $\mu$ M Dofetilide (Fig. 9B).

#### **Intergraded effect of PD-307243 on hERG current during an action potential**

Since PD-307243 affected multiple properties of hERG channels, we wanted to evaluate the overall effect of PD-307243 on hERG currents during an action potential. For this purpose we used a voltage-clamp protocol modeled on an action potential prerecorded from a rabbit ventricular myocyte (Fig. 10A). The current trace was recorded in CHO cells expressing hERG channels before (control in Fig. 10B) and after 3  $\mu$ M PD-307243 perfusion with repetitive stimuli at 5-s interval. The trace labeled as 3  $\mu$ M PD-307243 was recorded when the drug response reached steady-state (Fig. 10B). The shape of the hERG current resembled the action potential. Measurement of the area under the hERG current trace in control and in the presence of 3  $\mu$ M PD-307243 revealed that there was an  $8.8 \pm 1.0$  fold ( $n=5$ ) increase in the total potassium ions conducted by hERG channels during the action potential in the presence of the compound.



### **Action of PD-307243 on other cardiac ion channels**

We next wanted to examine the specificity of action of PD-307243, and tested it on a range of known cardiac ion channels. We tested the action of PD-307243 on the KCNQ1+minK complex heterologously expressed in CHO cells, the molecular correlate of  $I_{Ks}$  (Sanguinetti *et al.*, 1996). At a concentration of 3  $\mu$ M, PD-307243 significantly increased KCNQ1+minK current,  $64\pm 12\%$  ( $n=5$ ) at +50 mV (Supplemental Fig. 1). PD-307243 was also found to activate L-type  $Ca^{2+}$  current recorded in ventricular myocytes isolated from rabbit hearts. At concentrations of 3 and 10  $\mu$ M, PD-307243 increased peak  $Ca^{2+}$  current recorded at +10 mV by  $29\pm 4\%$  ( $n=6$ ) and  $52\pm 11\%$  ( $n=5$ ), respectively (Supplemental Fig. 2); the increases were statistically significant. PD-307243 (3  $\mu$ M) had no effect on  $I_{to}$  recorded from ventricular myocytes (Supplemental Fig. 3) or human  $Na_v1.5$  channels heterologously expressed in HEK 293 cells (Supplemental Fig. 4).

### **PD-307243 docks in the extracellular mouth of the pore**

A model of the hERG channel incorporating the extracellular S5, P and S6 segments was constructed. This was based initially on its homology with a mammalian Shaker family potassium channel (Kv1.2), but the S5-P loop regions were subsequently modified in accordance with details described in a recent publication (Tseng *et al.*, 2007). The important aspects of the biophysical studies that have been applied to the model are as follows: residues 576-583 and 585-594 are most likely to adopt an amphipathic alpha helical structure; the hydrophobic residues on the S5-P2 helix are in high impact positions oriented towards the internal face of the hERG channel, with the hydrophilic residues facing the solvent front. Following geometry optimization of the

## MOL #41152

protein receptor model, the hERG channel activator PD-370243 was docked in the extracellular portion of the molecule, with the docking grid loosely defined around the center of the pore. The docking was performed using Glide under standard SP conditions, with the top ten scoring poses being retained. All ten poses were oriented in a similar manner, with the carboxylic acid moiety pointed towards the center of the pore and interacting with the side-chain hydroxyl group of Serine 631, as shown in Fig. 11. The hydrophobic domains of the small molecule, primarily the dichlorophenyl moiety, are making positive interactions with the lipophilic residues Leucine 589 and Isoleucine 593 of the protein. This orientation is consistent with the limited structure-activity data for this compound (Zhou *et al.*, 2005), highlighting the importance of the carboxylic acid moiety and hydrophobic domain to the activity of this molecule.

## **Discussion**

In this study, we demonstrated that PD-307243 concentration-dependently increased hERG currents and elucidated its mode of action. Here we show for the first time that PD-307243 has a site of action close to the extracellular mouth of the channel pore.

PD-307243 induced persistent hERG current at very negative membrane potentials and  $I_{to}$ -like hERG current followed by a rising phase at positive voltages. The generation of the instantaneous current at all the voltages is attributable to dramatic slowing of channel deactivation, with some channels being perpetually held in an open state even at very negative membrane potentials. Since hERG channel inactivation is quite limited at negative voltages ( $\leq -60$  mV), the hERG current shows little decay. At more positive voltages, hERG channel inactivation becomes more apparent. Since PD-307243 dramatically slowed the onset of hERG current inactivation, a clear cut inactivating phase of hERG current was observed at depolarization steps which is absent under normal circumstances due to very fast hERG channel inactivation (Kiehn *et al.*, 1999; Zhou *et al.*, 1998). The slowly rising phase of hERG current after initial decay reflects the opening of additional hERG channels in the close state in response to membrane depolarization.

The induction of the instantaneous hERG current by PD-307243 requires channel opening, this is consistent with the observation made for RPR260243 (Kang *et al.*, 2005), a hERG channel activator which mainly slows hERG channel deactivation

## MOL #41152

without affecting other channel properties. The  $I_{to}$ -like current appears at the 2<sup>nd</sup> pulse after RPR260243 treatment and the amplitude of the instantaneous hERG current is unchanged with continuous pulsing. In contrast, the binding of PD-307243 to the hERG channel seems to be use-dependent. With continuous stimulation, more and more hERG channels are accumulated at open state due to incomplete deactivation, resulting in increasing  $I_{to}$ -like current amplitude. This use-dependent action of PD-307243 strongly implies that the site of action of the compound may be within the channel pore and only becomes accessible on channel opening. The reversal potential of the hERG current is not altered in the presence of the drug and this argues against it modulating the channel by interacting with the selectivity filter.

Extracellular application of PD-307243 gives a small rightward shift in  $V_{1/2}$  for voltage-dependent recovery from inactivation. This property is consistent with other reported hERG channel activators, such as Mallotoxin (Zeng *et al.*, 2006), NS1643 and NS3623 (Hansen *et al.*, 2006a; Hansen *et al.*, 2006b). However, the small shift was not observed for NS1643 in another study (Casis *et al.*, 2006). In addition, PD-307243 dramatically slows the onset of hERG current inactivation. Although NS1643 (Casis *et al.*, 2006) and NS3623 (Hansen *et al.*, 2006b) also slow the rate of hERG current inactivation, these drug did not change the characteristic acceleration of inactivation with more depolarized membrane potentials. In the presence of PD-307243, hERG current inactivates much slower at more positive voltages. The slowing of time-dependent inactivation coupled with the retarded channel closure generates the  $I_{to}$ -like hERG current at positive membrane potentials.

Our experimental findings suggest that PD-307243 acts on the outer regions of the channel pore leading to the modification of inactivation gating. The extracellular turret and the pore loop are important for channel inactivation (Witchel, 2007). Particularly, amino acid residues 583-597, have been identified to play a critical role in the C-type inactivation of hERG channel (Liu *et al.*, 2002; Torres *et al.*, 2003; Jiang *et al.*, 2005). In fact, a mutation resulting in an asparagine to lysine substitution at position 588 (N588K) is associated with an inherited form of SQTS, which is characterized by a significant slowing of channel inactivation (Cordeiro *et al.*, 2005; McPate *et al.*, 2005).

Leu589 and Ile593 have previously been reported to play important roles in hERG channel inactivation (Jiang *et al.*, 2005; Liu *et al.*, 2002; Torres *et al.*, 2003); docking studies suggest that PD-307243 binds in the extracellular region of the channel pore and shows points of contact with these two residues. Additionally, the carboxylic acid moiety of PD-307243 was shown to form a hydrogen bond with the serine residue at position 631. A mutation of this residue to an alanine impairs, but does not abolish channel inactivation (Zou *et al.*, 1998), which appears to be consistent with the action of PD-307243.

It is plausible that binding of the compound to the extracellular region of the channel pore leads to conformational changes in the channel which ultimately results in the impaired deactivation that is observed. The slowing of channel deactivation that is observed in the inside-out configuration can therefore result from two scenarios. The

first could involve the binding of PD-307243 to a low affinity site on the intracellular side of the channel pore that attenuates channel deactivation. In the second instance there could be a slow diffusion of the compound to the extracellular binding site, and the identified difference that we observe on channel inactivation compared to that seen in the whole cell mode could be explained by the accumulation of low concentrations at the site of action.

Although hERG activators RPR260243 (Kang *et al.*, 2005), NS1643 (Hansen *et al.*, 2006a), NS3623 (Hansen *et al.*, 2006b) and PD-118057 (Zhou *et al.*, 2005) have been shown to shorten cardiac action potential, only RPR260243 has been tested on  $I_{Kr}$  in native cells. As seen in the hERG channels expressed in CHO cells, RPR260243 slows  $I_{Kr}$  deactivation in guinea pig ventricular myocytes (Kang *et al.*, 2005). We also clearly demonstrated that  $I_{Kr}$  activated by PD-307243 in rabbit ventricular myocytes had an upstroke followed by inactivation as seen in CHO cells expressing hERG channels, though less dramatic. This confirms that the effects of PD-307243 on the deactivation and inactivation properties of hERG channels is not limited to the heterologous expression system but is reproducible in native channels passing  $I_{Kr}$  in ventricular myocytes.

The observations that hERG channel deactivation and inactivation are greatly altered in the presence of the compound can also explain the hERG current profile during an action potential. In the presence of the drug, hERG channels become constitutive and lose characteristic rectification. Therefore, the hERG current more or less passively

followed the membrane potential. hERG channel gating is suited for the role it plays in driving phase III of the ventricular action potential, rapid inactivation rendering the channels unable to conduct potassium ions during phase II of the action potential (Vandenberg *et al.*, 2004; Witchel, 2007). If this was altered it could have consequences on the generation of other ion channel currents. We postulate that the instantaneous  $I_{Kr}$  observed in the presence of PD-307243 could prematurely terminate the action potential of ventricular myocytes and be potentially proarrhythmic, provided PD-307243 is a selective hERG ( $I_{Kr}$ ) activator. It should be noted that activators of hERG have been shown to shorten the QT interval (Zhou *et al.*, 2005; Kang *et al.*, 2005). Therefore, the mechanisms by which small molecule activation of hERG channels occur need to be carefully studied in the search for activators that will optimally modify the action potential repolarization in patients with LQTS. The non-specific nature of activities of PD-307243 on a number of cardiac ion channels that are known to play important roles in the genesis and maintenance of the ventricular action potential renders PD-307243 inappropriate to demonstrate the effect of  $I_{Kr}$  activation on action potential shortening. Activation of  $I_{Kr}$  and L-type  $Ca^{2+}$  currents would offset each other and make the action potential data difficult to interpret.

Taken together the results of this study reveal that hERG channel activation by PD-307243 might be the result of its binding in the extracellular region of the pore. The compound modifies channel inactivation and also retards deactivation holding the channel in a constitutively open state. Our findings provide the basis for further studies

## **MOL #41152**

that will not only be useful in the rational design of hERG channel openers, but could also be critical for the elimination of unwanted effects due to hERG channel activation.



Reference

Abbott GW, Sesti F, Splawski I, Buck M E, Lehmann M H, Timothy K W, Keating M T and Goldstein S A (1999) MiRP1 Forms IKr Potassium Channels With HERG and Is Associated With Cardiac Arrhythmia. *Cell* **97**: 175-187.

Brown AM (2005) HERG Block, QT Liability and Sudden Cardiac Death. *Novartis Found Symp* **266**: 118-131.

Brugada R, Hong K, Dumaine R, Cordeiro J, Gaita F, Borggrefe M, Menendez T M, Brugada J, Pollevick G D, Wolpert C, Burashnikov E, Matsuo K, Wu Y S, Guerchicoff A, Bianchi F, Giustetto C, Schimpf R, Brugada P and Antzelevitch C (2004) Sudden Death Associated With Short-QT Syndrome Linked to Mutations in HERG. *Circulation* **109**: 30-35.

Casis O, Olesen S P and Sanguinetti M C (2006) Mechanism of Action of a Novel Human Ether-a-Go-Go-Related Gene Channel Activator. *Mol Pharmacol* **69**: 658-665.

Cordeiro JM, Brugada R, Wu Y S, Hong K and Dumaine R (2005) Modulation of I(Kr) Inactivation by Mutation N588K in KCNH2: a Link to Arrhythmogenesis in Short QT Syndrome. *Cardiovasc Res* **67**: 498-509.

Hansen RS, Diness T G, Christ T, Demnitz J, Ravens U, Olesen S P and Grunnet M (2006a) Activation of Human Ether-a-Go-Go-Related Gene Potassium Channels by the Diphenylurea 1,3-Bis-(2-Hydroxy-5-Trifluoromethyl-Phenyl)-Urea (NS1643). *Mol Pharmacol* **69**: 266-277.

Hansen RS, Diness T G, Christ T, Wettwer E, Ravens U, Olesen S P and Grunnet M (2006b) Biophysical Characterization of the New Human Ether-a-Go-Go-Related Gene Channel Opener NS3623 [N-(4-Bromo-2-(1H-Tetrazol-5-Yl)-Phenyl)-N'-(3'-Trifluoromethylphenyl)Urea ]. *Mol Pharmacol* **70**: 1319-1329.

Jiang M, Zhang M, Maslennikov I V, Liu J, Wu D M, Korolkova Y V, Arseniev A S, Grishin E V and Tseng G N (2005) Dynamic Conformational Changes of Extracellular S5-P Linkers in the HERG Channel. *J Physiol* **569**: 75-89.

Jurkiewicz NK and Sanguinetti M C (1993) Rate-Dependent Prolongation of Cardiac Action Potentials by a Methanesulfonanilide Class III Antiarrhythmic Agent. Specific Block of Rapidly Activating Delayed Rectifier K<sup>+</sup> Current by Dofetilide. *Circ Res* **72**: 75-83.

Kang J, Chen X L, Wang H, Ji J, Cheng H, Incardona J, Reynolds W, Viviani F, Tabart M and Rampe D (2005) Discovery of a Small Molecule Activator of the Human Ether-a-Go-Go-Related Gene (HERG) Cardiac K<sup>+</sup> Channel. *Mol Pharmacol* **67**: 827-836.

Kiehn J, Lacerda A E and Brown A M (1999) Pathways of HERG Inactivation. *Am J Physiol* **277**: H199-H210.

Lalik PH, Krafft D S, Volberg W A and Ciccarelli R B (1993) Characterization of Endogenous Sodium Channel Gene Expressed in Chinese Hamster Ovary Cells. *Am J Physiol* **264**: C803-C809.

Liu J, Zhang M, Jiang M and Tseng G N (2002) Structural and Functional Role of the Extracellular S5-p Linker in the HERG Potassium Channel. *J Gen Physiol* **120**: 723-737.

Long SB, Campbell E B and Mackinnon R (2005) Crystal Structure of a Mammalian Voltage-Dependent Shaker Family K<sup>+</sup> Channel. *Science* **309**: 897-903.

McPate MJ, Duncan R S, Milnes J T, Witchel H J and Hancox J C (2005) The N588K-HERG K<sup>+</sup> Channel Mutation in the 'Short QT Syndrome': Mechanism of Gain-in-Function Determined at 37 Degrees C. *Biochem Biophys Res Commun* **334**: 441-449.

Micheli F, Bonanomi G, Blaney F E, Braggio S, Capelli A M, Checchia A, Curcuruto O, Damiani F, Fabio R D, Donati D, Gentile G, Gribble A, Hamprecht D, Tedesco G, Terreni S, Tarsi L, Lightfoot A, Stemp G, Macdonald G, Smith A, Pecoraro M, Petrone M, Perini O, Piner J, Rossi T, Worby A, Pilla M, Valerio E, Griffante C, Mugnaini M, Wood M, Scott C, Andreoli M, Lacroix L, Schwarz A, Gozzi A, Bifone A, Ashby C R, Jr., Hagan J J and Heidbreder C (2007) 1,2,4-Triazol-3-yl-thiopropyl-Tetrahydrobenzazepines: a Series of Potent and Selective Dopamine D(3) Receptor Antagonists. *J Med Chem* **50**: 5076-5089.

Modell SM and Lehmann M H (2006) The Long QT Syndrome Family of Cardiac Ion Channelopathies: a HuGE Review. *Genet Med* **8**: 143-155.

Rials SJ, Wu Y, Xu X, Filart R A, Marinchak R A and Kowey P R (1997) Regression of Left Ventricular Hypertrophy With Captopril Restores Normal Ventricular Action Potential Duration, Dispersion of Refractoriness, and Vulnerability to Inducible Ventricular Fibrillation. *Circulation* **96**: 1330-1336.

Sanguinetti MC, Curran M E, Zou A, Shen J, Spector P S, Atkinson D L and Keating M T (1996) Coassembly of K(V)LQT1 and MinK (IsK) Proteins to Form Cardiac I(Ks) Potassium Channel. *Nature* **384**: 80-83.

Seeböhm G (2005) Activators of Cation Channels: Potential in Treatment of Channelopathies. *Mol Pharmacol* **67**: 585-588.

Smith PL, Baukrowitz T and Yellen G (1996) The Inward Rectification Mechanism of the HERG Cardiac Potassium Channel. *Nature* **379**: 833-836.

Spector PS, Curran M E, Zou A, Keating M T and Sanguinetti M C (1996) Fast Inactivation Causes Rectification of the IKr Channel. *J Gen Physiol* **107**: 611-619.

Torres AM, Bansal P S, Sunde M, Clarke C E, Bursill J A, Smith D J, Bauskin A, Breit S N, Campbell T J, Alewood P F, Kuchel P W and Vandenberg J I (2003) Structure of the HERG K<sup>+</sup> Channel S5P Extracellular Linker: Role of an Amphipathic Alpha-Helix in C-Type Inactivation. *J Biol Chem* **278**: 42136-42148.

Tseng GN, Sonawane K D, Korolkova Y V, Zhang M, Liu J, Grishin E V and Guy H R (2007) Probing the Outer Mouth Structure of the HERG Channel With Peptide Toxin Footprinting and Molecular Modeling. *Biophys J* **92**: 3524-3540.

Vandenberg JI, Torres A M, Campbell T J and Kuchel P W (2004) The HERG K<sup>+</sup> Channel: Progress in Understanding the Molecular Basis of Its Unusual Gating Kinetics. *Eur Biophys J* **33**: 89-97.

Wible BA, Hawryluk P, Ficker E, Kuryshev Y A, Kirsch G and Brown A M (2005) HERG-Lite: a Novel Comprehensive High-Throughput Screen for Drug-Induced HERG Risk. *J Pharmacol Toxicol Methods* **52**: 136-145.

Witchel HJ (2007) The HERG Potassium Channel As a Therapeutic Target. *Expert Opin Ther Targets* **11**: 321-336.

Yu SP and Kerchner G A (1998) Endogenous Voltage-Gated Potassium Channels in Human Embryonic Kidney (HEK293) Cells. *J Neurosci Res* **52**: 612-617.

Zeng H, Lozinskaya I M, Lin Z, Willette R N, Brooks D P and Xu X (2006) Mallotoxin Is a Novel Human Ether-a-Go-Go-Related Gene (HERG) Potassium Channel Activator. *J Pharmacol Exp Ther* **319**: 957-962.

Zeng H, Weiger T M, Fei H, Jaramillo A M and Levitan I B (2005) The Amino Terminus of Slob, Slowpoke Channel Binding Protein, Critically Influences Its Modulation of the Channel. *J Gen Physiol* **125**: 631-640.

Zhou J, Augelli-Szafran C E, Bradley J A, Chen X, Koci B J, Volberg W A, Sun Z and Cordes J S (2005) Novel Potent Human Ether-a-Go-Go-Related Gene (HERG) Potassium Channel Enhancers and Their in Vitro Antiarrhythmic Activity. *Mol Pharmacol* **68**: 876-884.

Zhou Z, Gong Q, Ye B, Fan Z, Makielski J C, Robertson G A and January C T (1998) Properties of HERG Channels Stably Expressed in HEK 293 Cells Studied at Physiological Temperature. *Biophys J* **74**: 230-241.

**MOL #41152**

Zou A, Xu Q P and Sanguinetti M C (1998) A Mutation in the Pore Region of HERG K<sup>+</sup> Channels Expressed in *Xenopus* Oocytes Reduces Rectification by Shifting the Voltage Dependence of Inactivation. *J Physiol* **509 ( Pt 1)**: 129-137.

### Figure Legends

Figure 1. Time course of hERG channel activation by PD-307243 in CHO cells. Whole-cell currents were generated from a holding voltage of -80 mV with a single step to +20 mV for 2-s, followed by a tail pulse at -50 mV for 2-s. The protocol (inset) was repeated every 10-s. (A) Upper panel: Exemplar current traces of control and after 1, 2, and 4-min external perfusion with PD-307243 (10  $\mu$ M), generated with constant pulsing. Lower panel: Time course of current amplitude measured at the beginning of +20 mV step (I, Intermediate current), the last 100-ms of +20 mV step (S, Step current), peak current at returning to -50 mV (T, Tail peak current). Extracellular perfusion with PD-307243 was indicated by a horizontal bar. (B) Upper panel: Exemplar current traces of control and the first, second and twenty-fourth trace induced by constant pulsing after 4 minutes and 30 seconds of external perfusion with PD-307243 (10  $\mu$ M) without pulsing. Lower panel: Time course of instantaneous current (I), step current (S) and tail peak current (T). Inset: Chemical structure of PD-307243.

Figure 2. Effects of PD-307243 on the I-V of hERG channels in CHO cells. Whole-cell currents were generated from a holding voltage of -80 mV and stepped to a range of voltages between -60 mV and +80 mV in 10-mV increments for 2-s, followed by a tail pulse at -50 mV for 2-s. Inter-pulse interval was 10-s. (A) Exemplar traces showing the effect of PD-307243 (10  $\mu$ M) on a family of currents. Left: control traces; middle: current traces after drug effects reached steady-state; right: current traces after drug washout. (B) From left to right, I-V for instantaneous current (I), step current (S) and tail peak current (T) in control, 10  $\mu$ M PD-307243 and after washout.

## MOL #41152

Figure 3. Concentration-dependent effects of PD-307243 on hERG channels in CHO cells. (A) Exemplar traces showing the effect of PD-307243 (3  $\mu$ M) on a family of currents. Whole-cell currents were generated from a holding voltage of -80 mV and stepped to a range of voltages between -100 mV and +80 mV in 10-mV increments for 2-s, followed by a tail pulse at -120 mV for 2-s. Inter-pulse interval was 10-s. (1) control traces; (2) current traces after drug effects reached steady-state; (3) current traces in the presence of 3  $\mu$ M PD-307243 + 1  $\mu$ M Dofetilide; (4) Dofetilide sensitive currents. (B) Mean I-V (n=5-8 cells) for instantaneous current (I), step current (S) and tail peak current (T) in control, 1, 3 and 10  $\mu$ M PD-307243.

Figure 4. Appearance of persistent hERG current in the presence of PD-307243 requires channel opening. (A) Exemplar traces showing the effect of PD-307243 (3  $\mu$ M) on a family of currents. Whole-cell currents were generated using the voltage protocol from Fig. 3A inset with testing steps from -100 mV to -40 mV. Left: control traces; middle: first group of traces induced after 6-min drug perfusion (pre-pulsing); right: a group of traces induced after constant pulsing using the voltage protocol shown in Fig. 1A inset (post-pulsing). (B) I-V for instantaneous current (I), step current (S) and tail peak current (T) in control, 3  $\mu$ M PD-307243 pre- and after-constant pulsing.

Figure 5. Influence of PD-307243 on deactivation and the reversal potential of hERG channels. (A) Whole-cell currents were generated from a holding voltage of -130 mV with a single step to +20 mV for 2-s, followed by a tail pulse at -130 mV for 2-min (Top). Middle: Exemplar current traces of control and the first two traces after 2-min perfusion



## MOL #41152

with PD-307243 (3  $\mu$ M), generated with constant pulsing. Bottom: The same traces showing the first 4.5-s to highlight the development of the  $I_{to}$ -like current in the second trace after perfusion with the compound. (B) Whole-cell currents were generated from a holding potential of -80 mV with a single step to +40 mV for 2-s, followed by tail currents recorded at voltages the range -120 mV to -40 mV for 2-s (inset). Exemplar traces for control (left panel) and after perfusion with 3  $\mu$ M PD-307243 (middle panel). Right panel: I-V of tail peak current recorded at various voltages for control (closed square) and after perfusion with 3  $\mu$ M PD-307243 (closed square).m

Figure 6. Effect of PD-307243 on voltage-dependent recovery from inactivation of hERG channels in CHO cells. Whole-cell currents were generated by a three step protocol (inset). From a holding potential of -80 mV, channels were allowed to inactivate at +80 mV for 500-ms, this was followed by stepping the membrane to a range of voltages between -130 mV and +80 mV in 10-mV increments for 15-ms, to allow recovery from inactivation, and this was followed by a tail pulse to +80 mV for 500-ms. (A) Exemplar traces recorded under control conditions and in the presence of PD-307243 (3  $\mu$ M). (B) Peak tail currents were normalized to the maximal peak tail current at -130 mV and plotted against voltages for the control and PD-307243 (n=5 cells). The curves were fitted with the Boltzmann function:  $I/I_{max}=1/(1+\exp[(V-V_{1/2})/k])$ . \*, p <0.05.

Figure 7. Effect of PD-307243 on the inactivation time constant of hERG current in CHO cells. (A) Exemplar traces showing the measurement of hERG current inactivation under control conditions and in the presence of PD-307243 (3  $\mu$ M). Whole-cell currents

## MOL #41152

were generated by a three step protocol. From a holding potential of -80 mV, channels were allowed to inactivate at +80 mV and then briefly allowed to recover at -130 mV for 15-ms, the membrane was then stepped to a range of voltages between -20 mV and +60 mV, in 20-mV increments. (B) The time constants obtained in the range of voltages -20 mV to +60 mV were plotted (n=4 cells). \*,  $p < 0.05$ .

Figure 8. Intracellular effect of PD-307243 on hERG channels expressed in CHO cells.

(A) Exemplar traces showing the current recorded in an inside-out patch in control, 3 and 10  $\mu\text{M}$  PD-307243, and after washout. Currents were evoked from a holding voltage of -80 mV, and stepped to +20 mV for 2-s followed by a tail current at -120 mV for 2-s. Inter-pulse interval was 10-s. (B) Exemplar traces showing the effect of PD-307243 at 3  $\mu\text{M}$  and 10  $\mu\text{M}$  in an inside-out patch on a family of currents. Currents were generated from a holding voltage of -80 mV and stepped to a range of voltages between -100 mV and +80 mV in 10-mV increments for 2-s, followed by a tail pulse at -120 mV for 2-s. Inter-pulse interval was 10-s. (C) Averaged I-V of tail peak current normalized by the tail current amplitude at +80 mV in control (n= 2-3 cells).

Figure 9. PD-307243 activates  $I_{K_r}$  in rabbit ventricular myocytes. (A) Whole-cell currents were generated from a holding potential of -80 mV and stepped to -30 mV, 0 mV and +30 mV for 1-s, followed by a tail pulse at -50 mV for 1-s. Inter-pulse interval was 10-s. Left: control current traces; middle: current traces in 3  $\mu\text{M}$  PD-307243 when drug response reached steady-state; right: the PD-307243 activated current obtained by subtracting the current traces on the left panel from those in the middle. (B) Same

## MOL #41152

voltage-clamp protocol as in panel A but only one step. Traces shown were the PD-307243 activated current before and after dofetilide (1  $\mu$ M) blockade.

Figure 10. PD-307243 increases total potassium ions conducted by hERG channels during an action potential stimulus. (A) A pre-recorded action potential trace was used as the voltage protocol to induce hERG currents. The protocol was repeated at 5-s interval. (B) hERG current traces before and after PD-307243 (3  $\mu$ M) application when drug effect reached steady-state.

Figure 11. PD-307243 docks in the extracellular regions of the channel pore. (A) hERG channel model with backbone cartoon representation, when red domains are alpha-helical and cyan domains are turns. The channel activator, PD-370243, is shown as a space filling model, colored by atom type. (B) The carboxylic acid moiety of the hERG channel activator, PD-370243, is shown interacting with the side-chain hydroxyl group of Serine 631. The conserved hydrophobic residues, W585, L586 and L589 are shown with their side-chains oriented towards the center of the pore channel. (C) The hERG channel model surface is colored by chemical nature, hydrophobic residues in green, hydrophilic residues in cyan, basic residues in blue and acidic residues in red. The pore channel is surrounded by hydrophobic residues at the mouth, where the more lipophilic domains of the activator are interacting, notably the dichlorophenyl moiety.

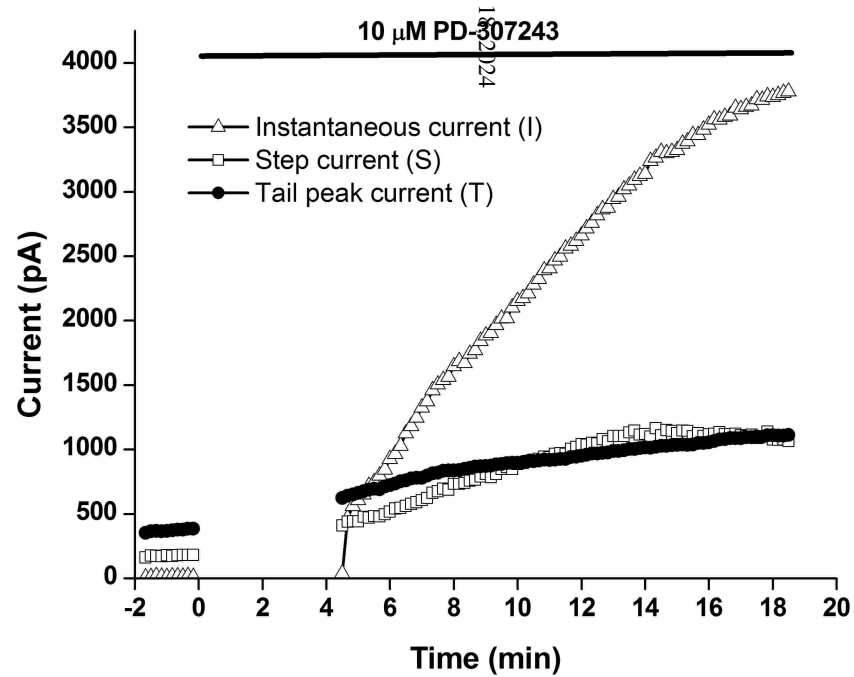
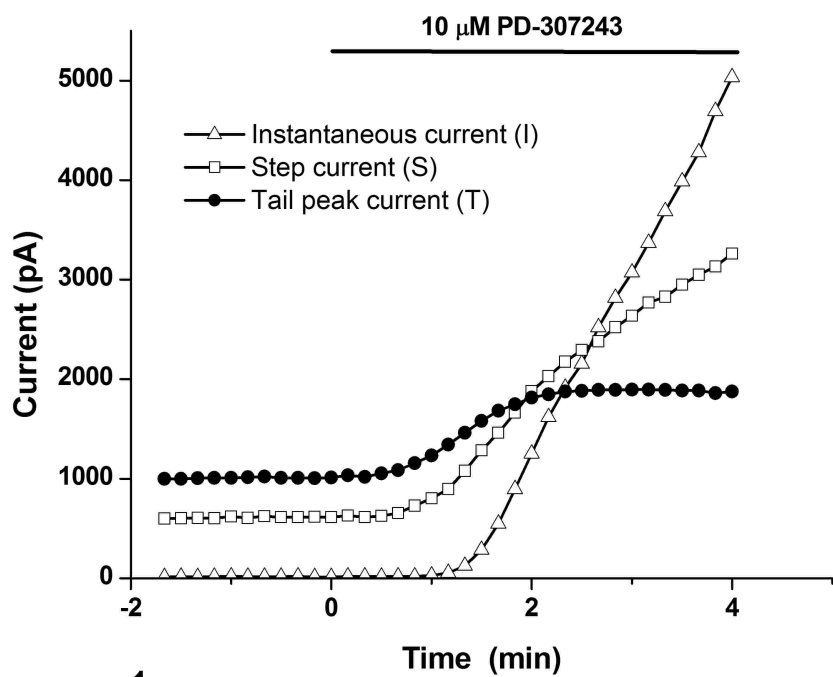
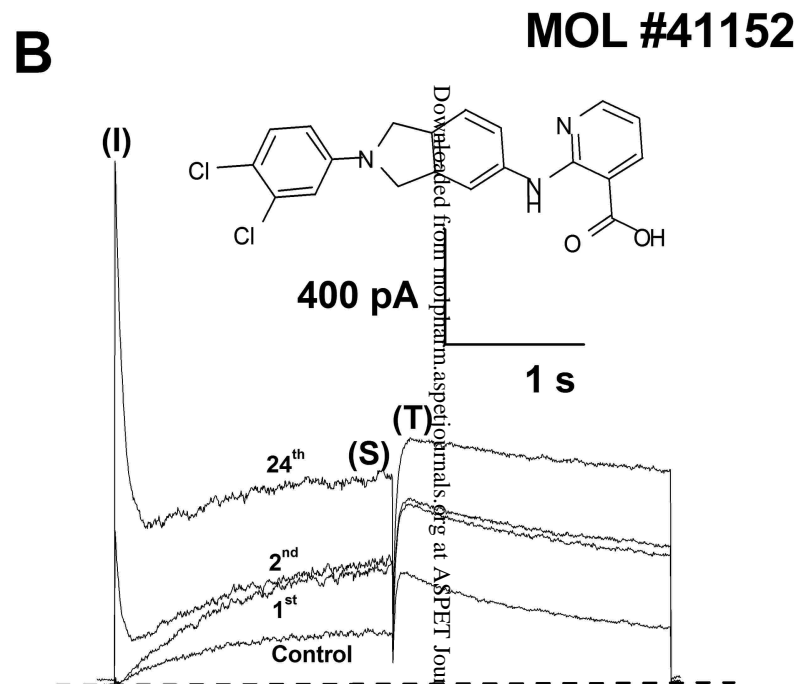
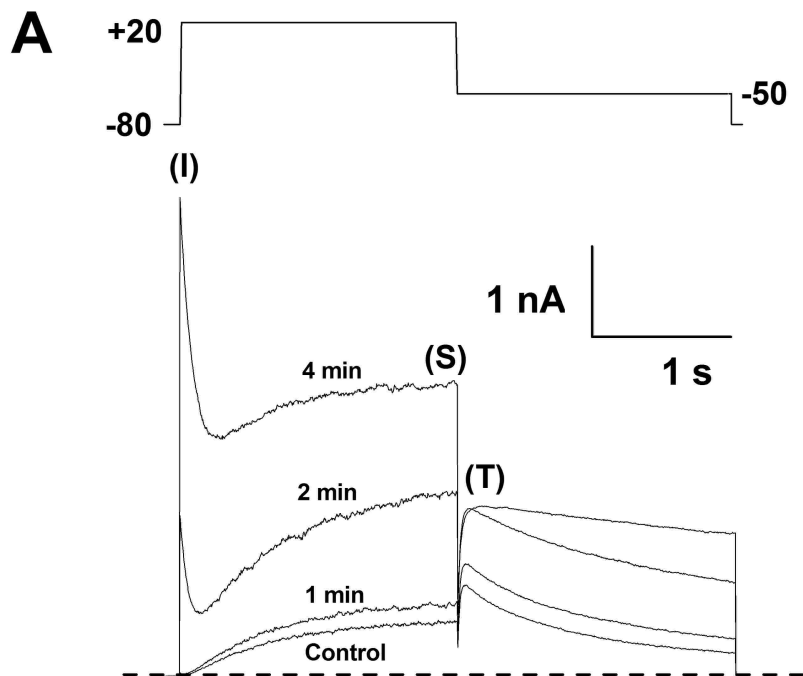
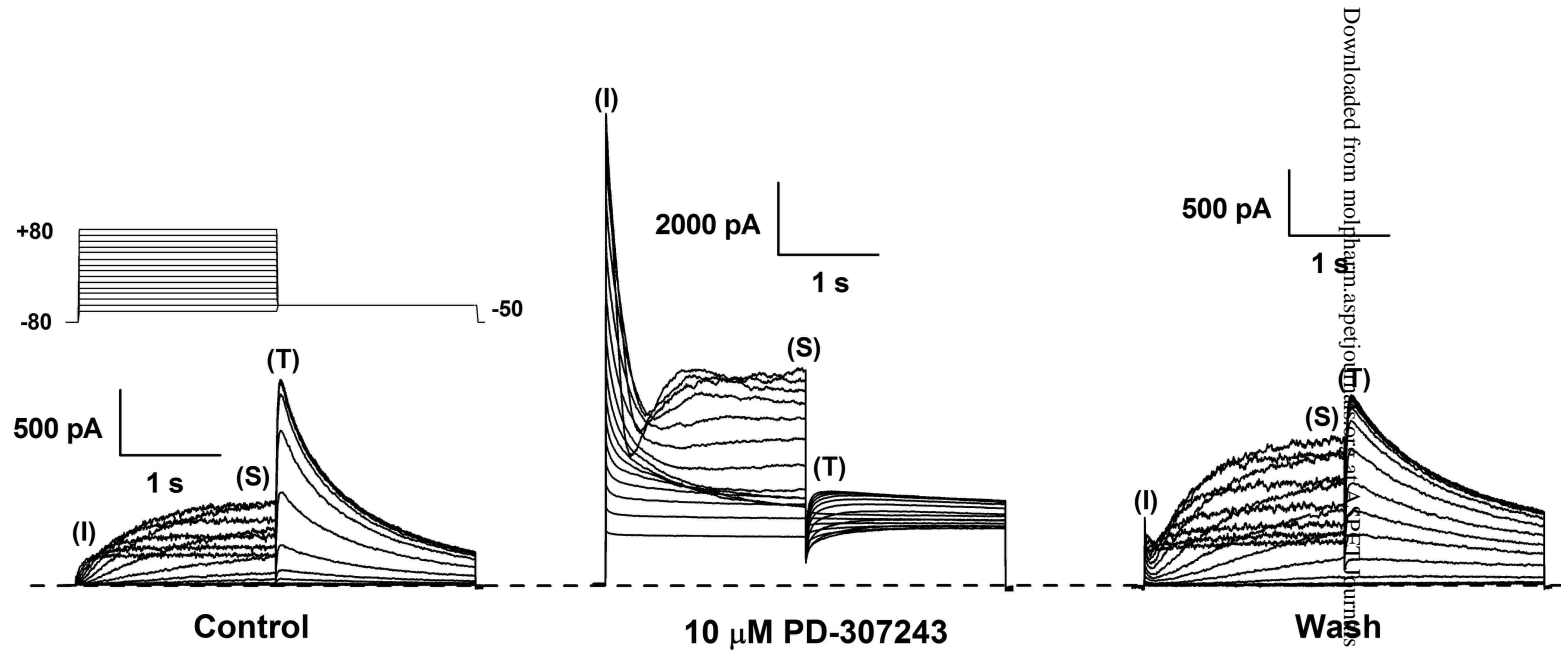


Figure 1

**A**



**B**

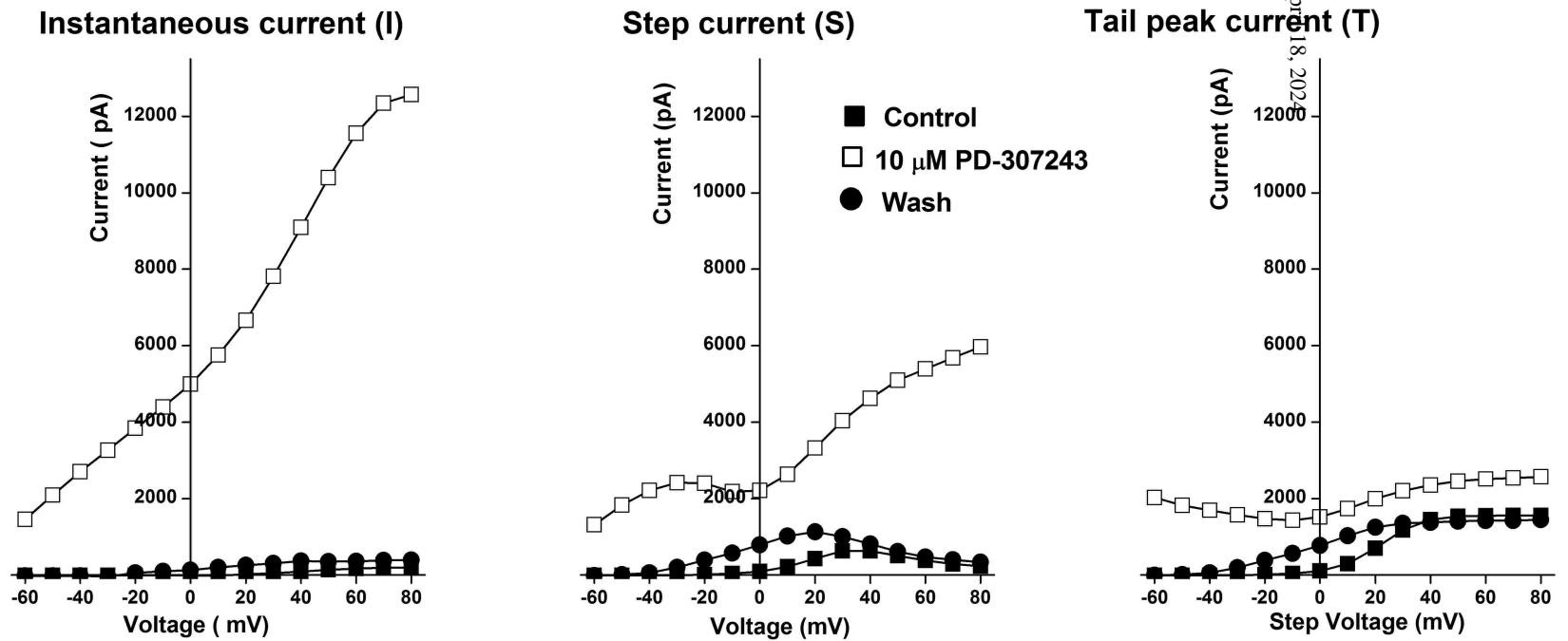
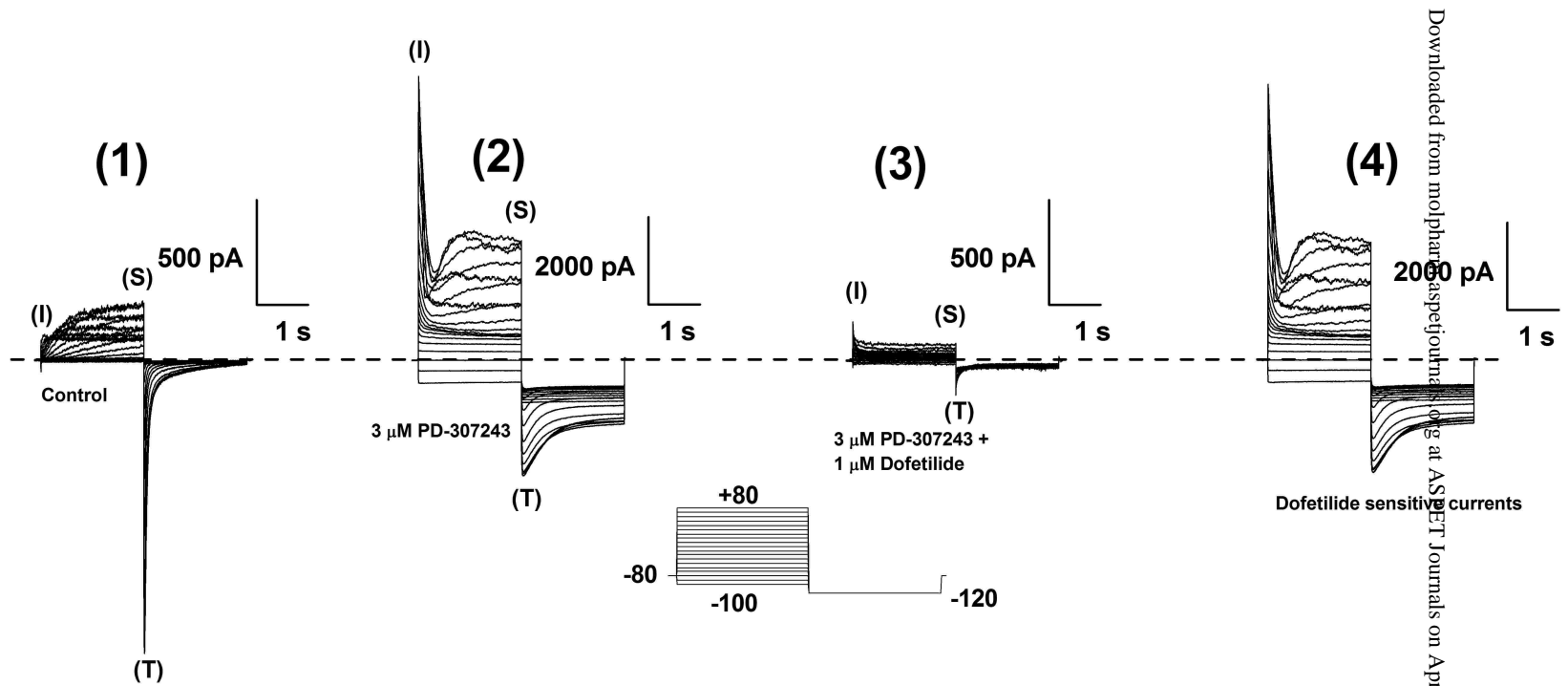


Figure 2

A



Downloaded from molpharm.aspetjournals.org at ASPET Journals on April 15, 2014

B

Instantaneous current (I)

Step current (S)

Tail peak current (T)

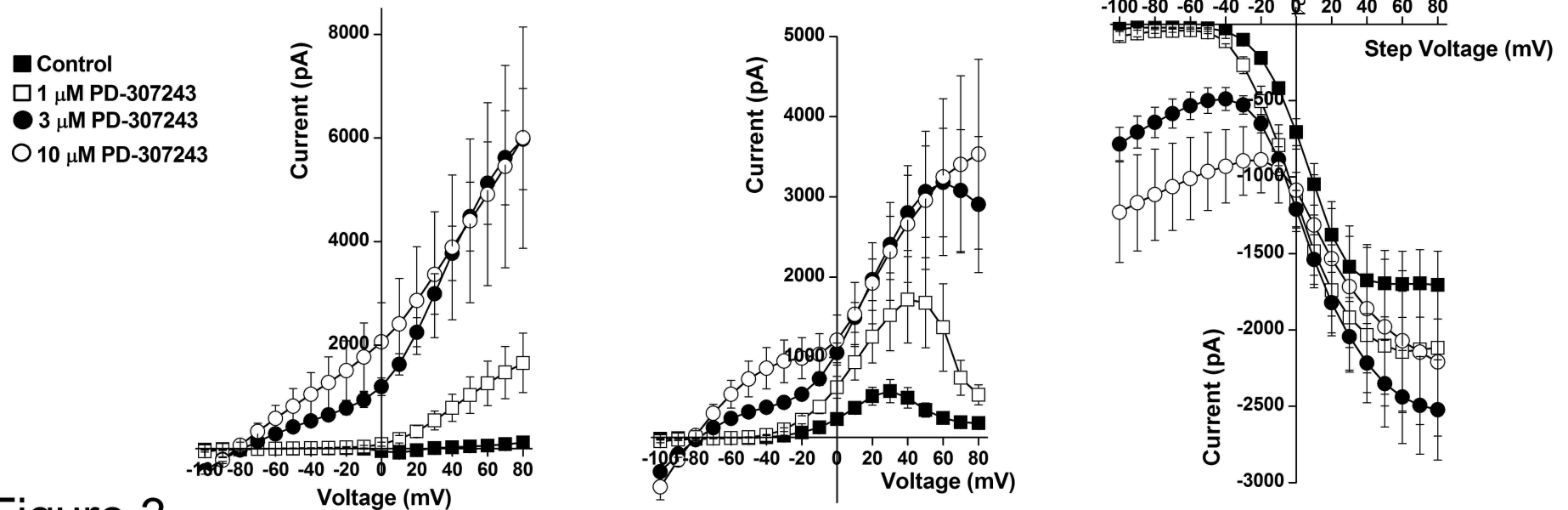


Figure 3

A



B

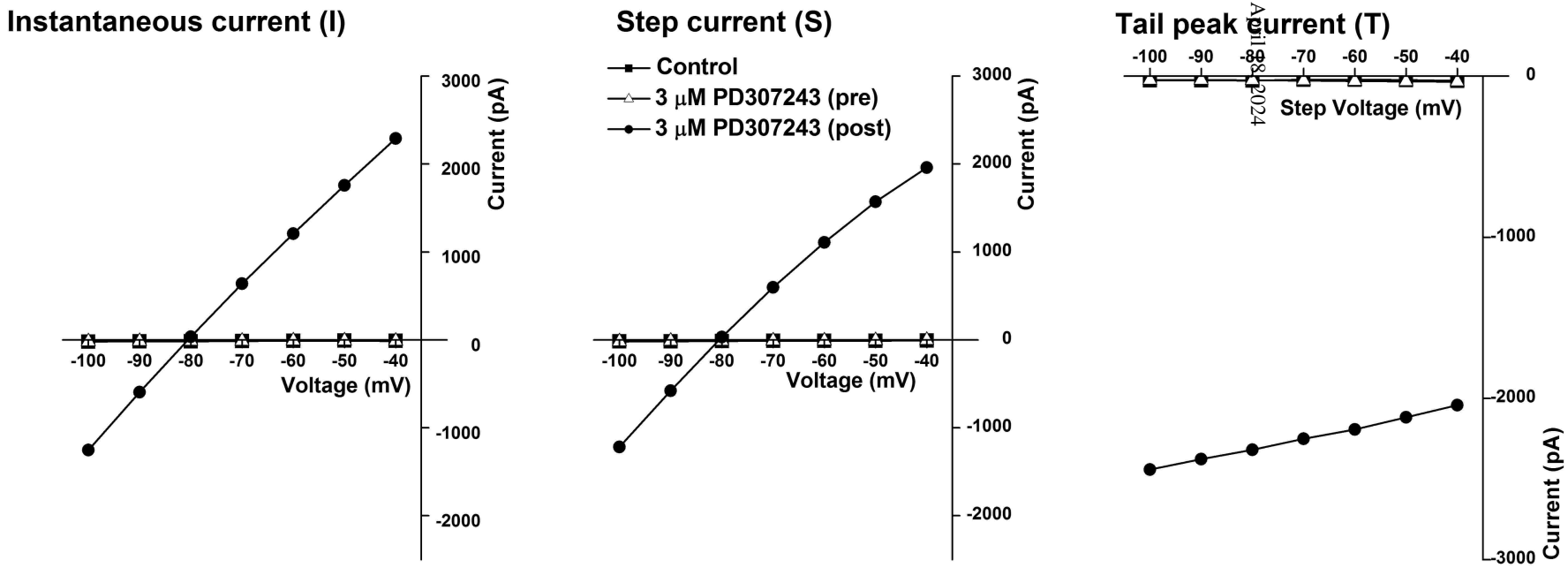
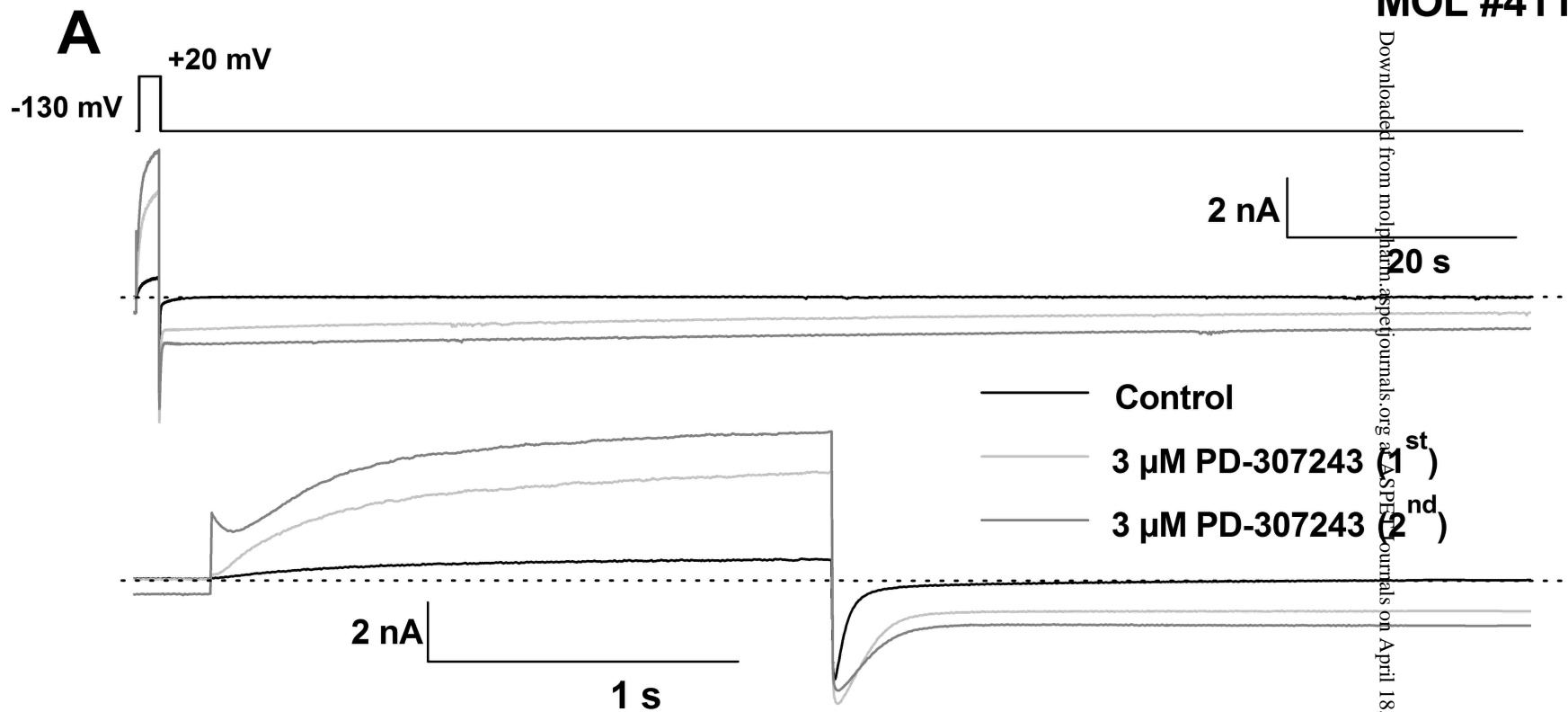


Figure 4



Downloaded from molpharm.aspetjournals.org at ASPET Journals on April 18, 2024

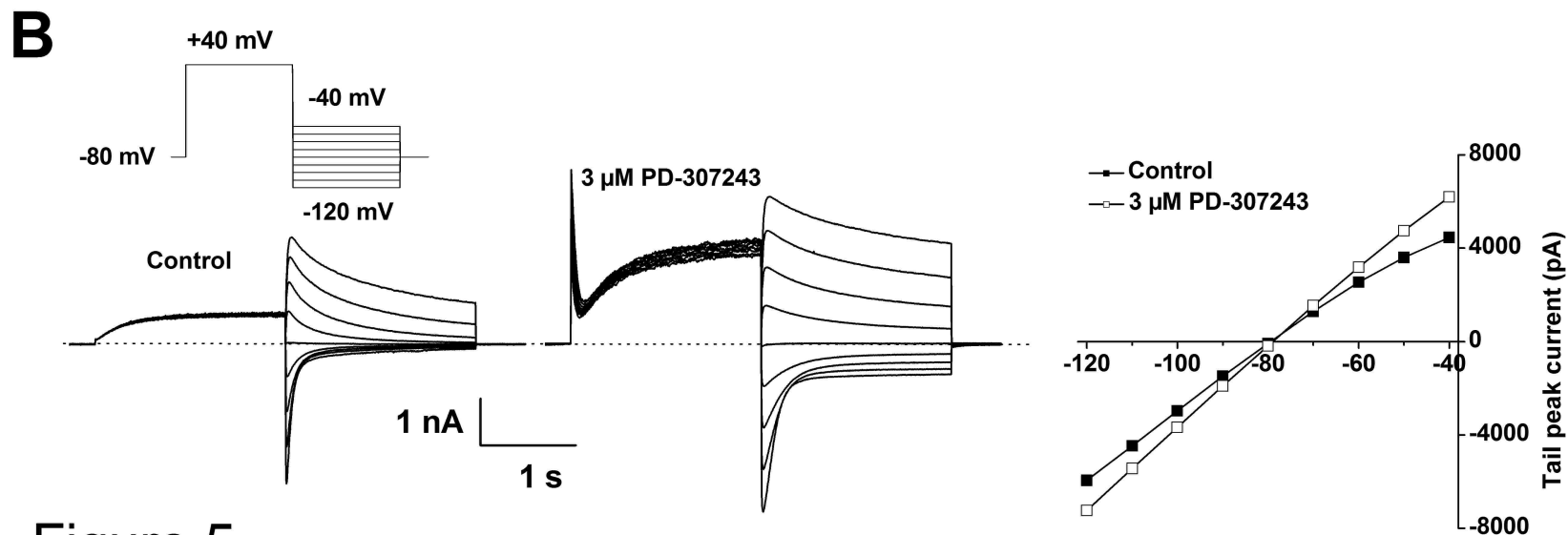
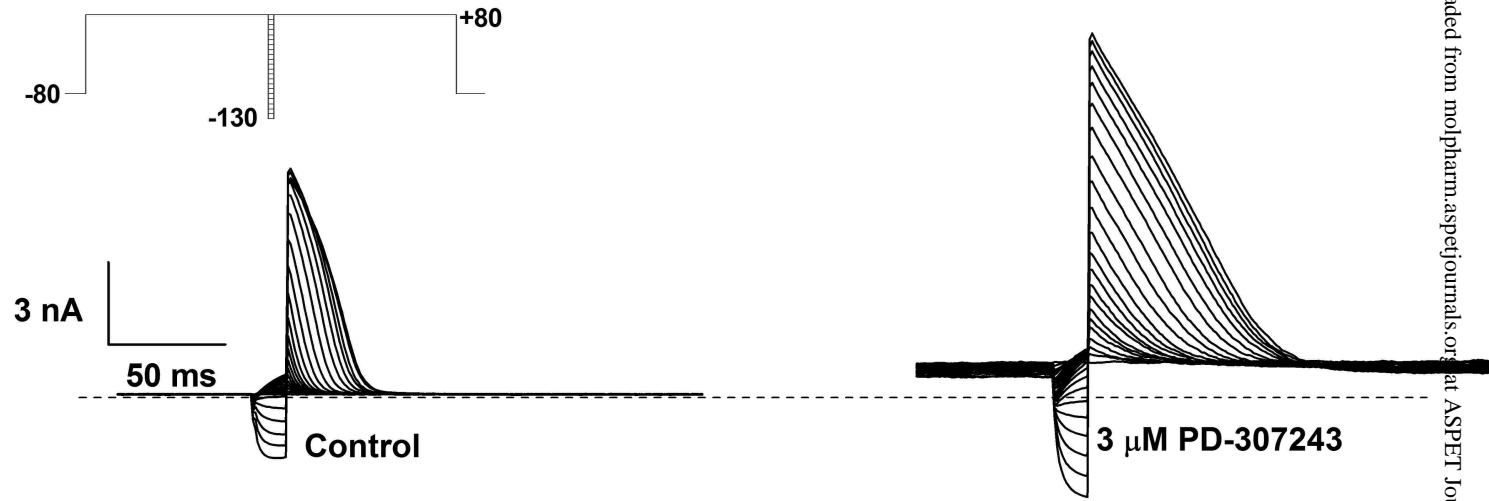


Figure 5



A



B

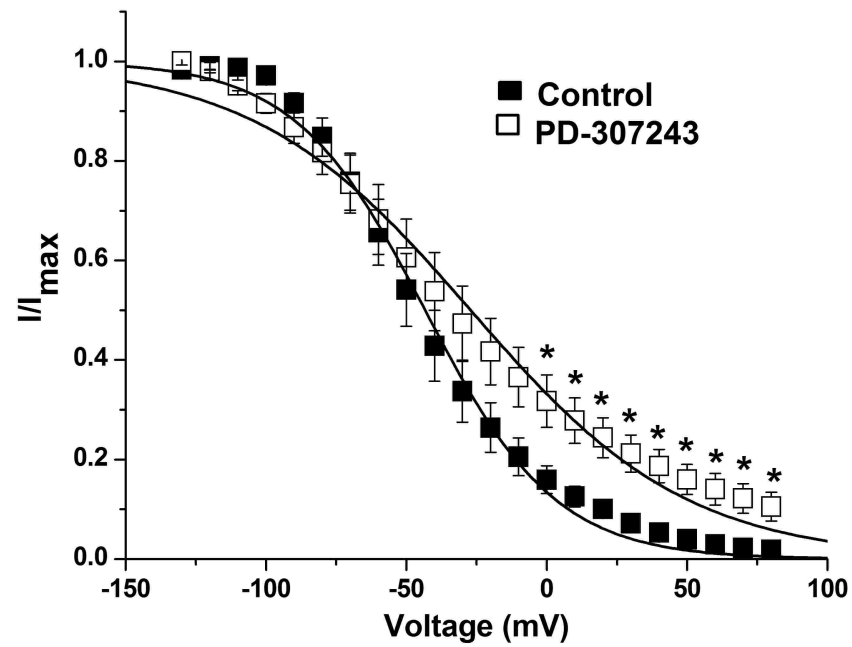
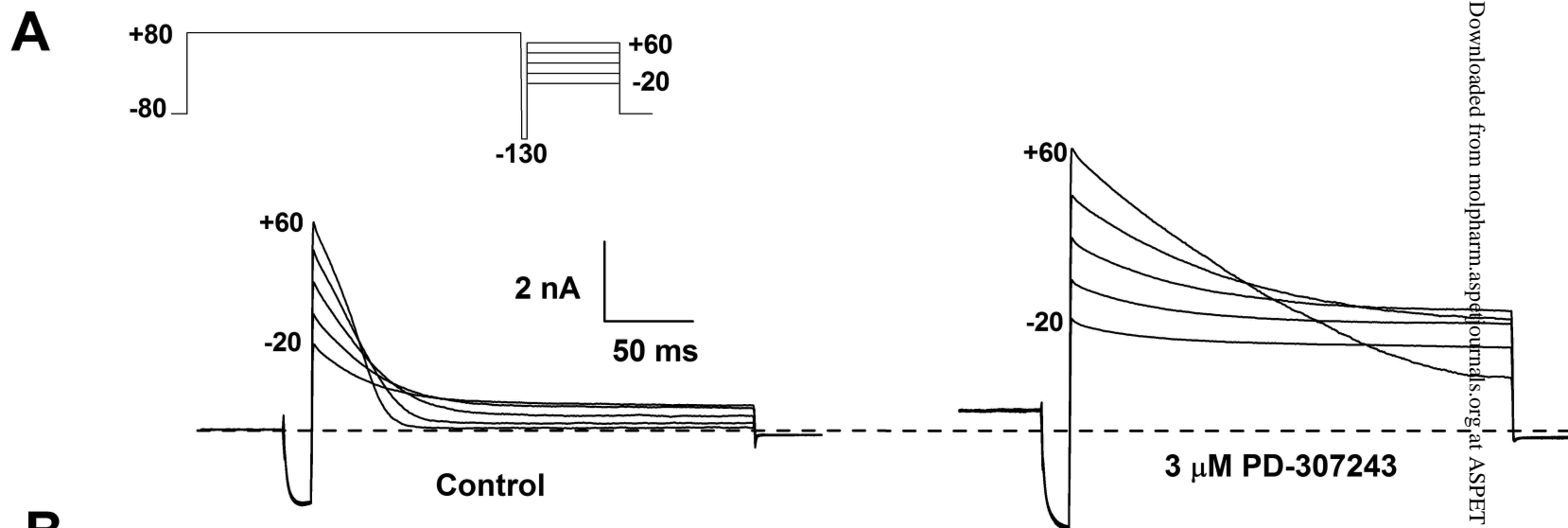


Figure 6



**B**

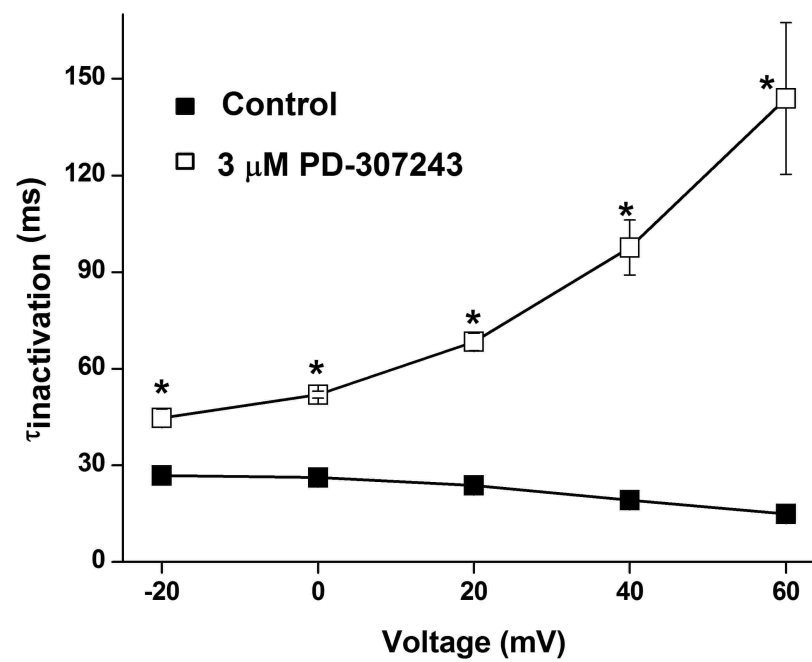


Figure 7

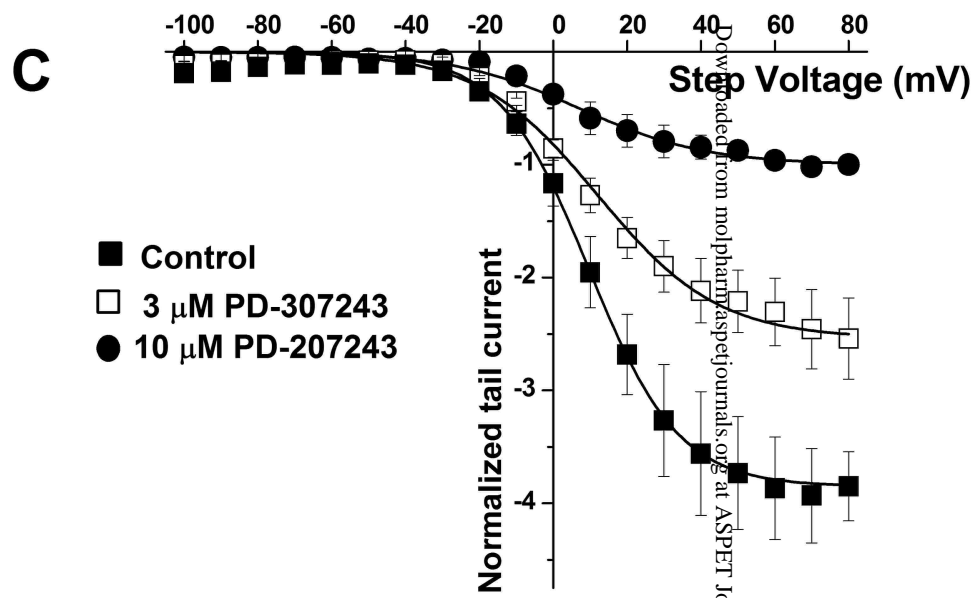
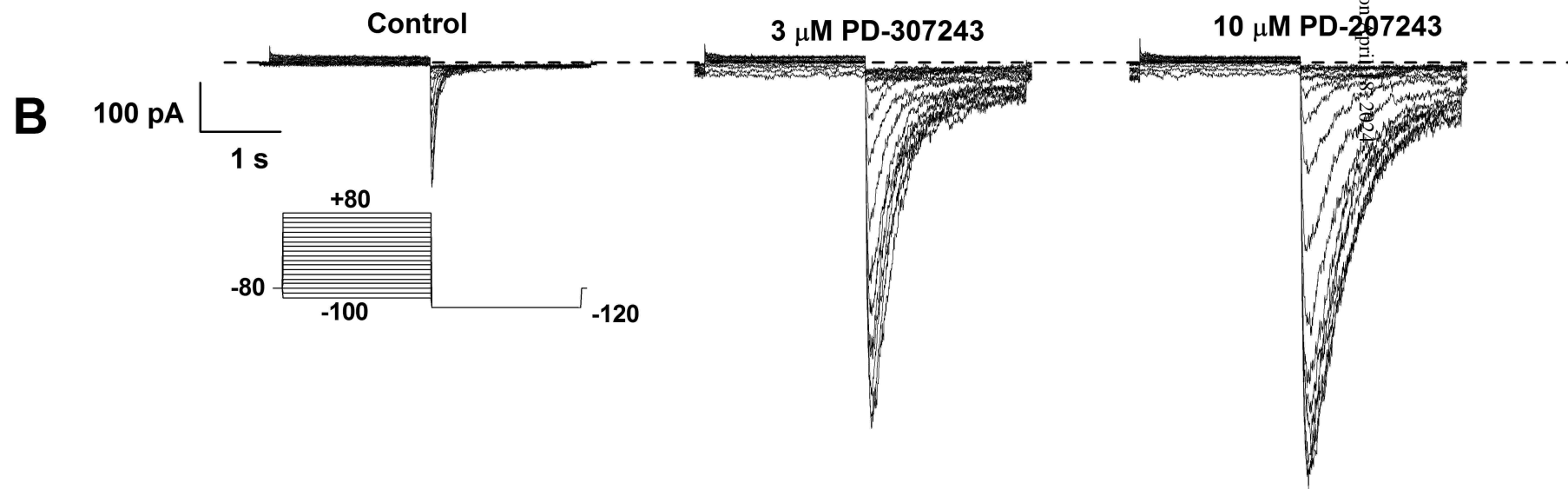
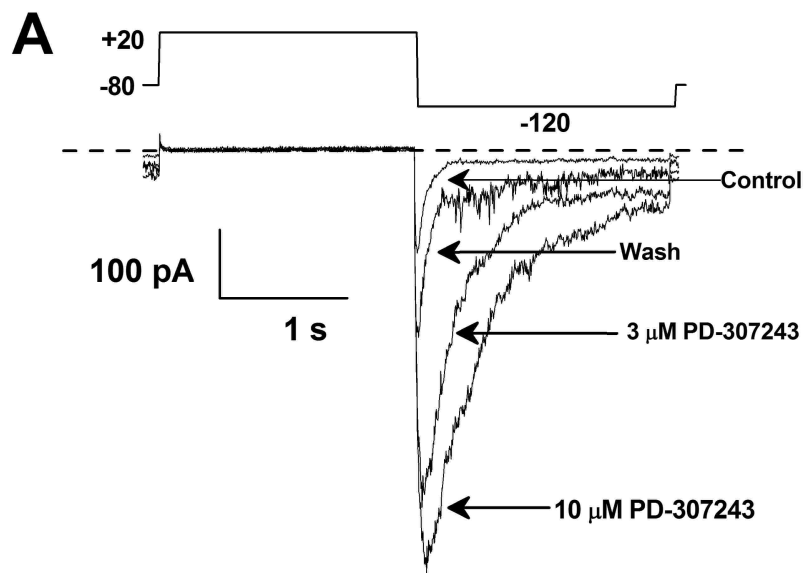


Figure 8

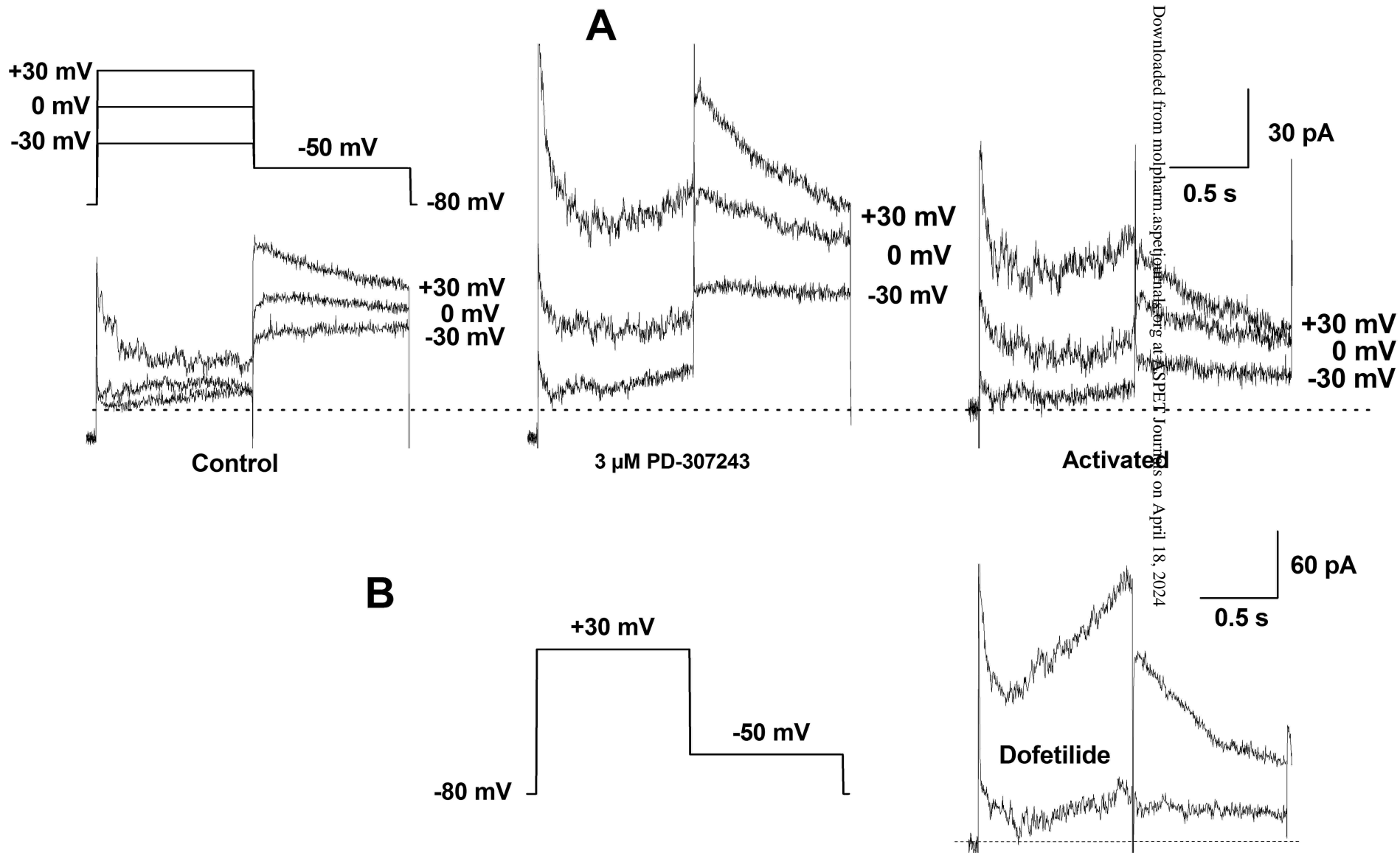


Figure 9

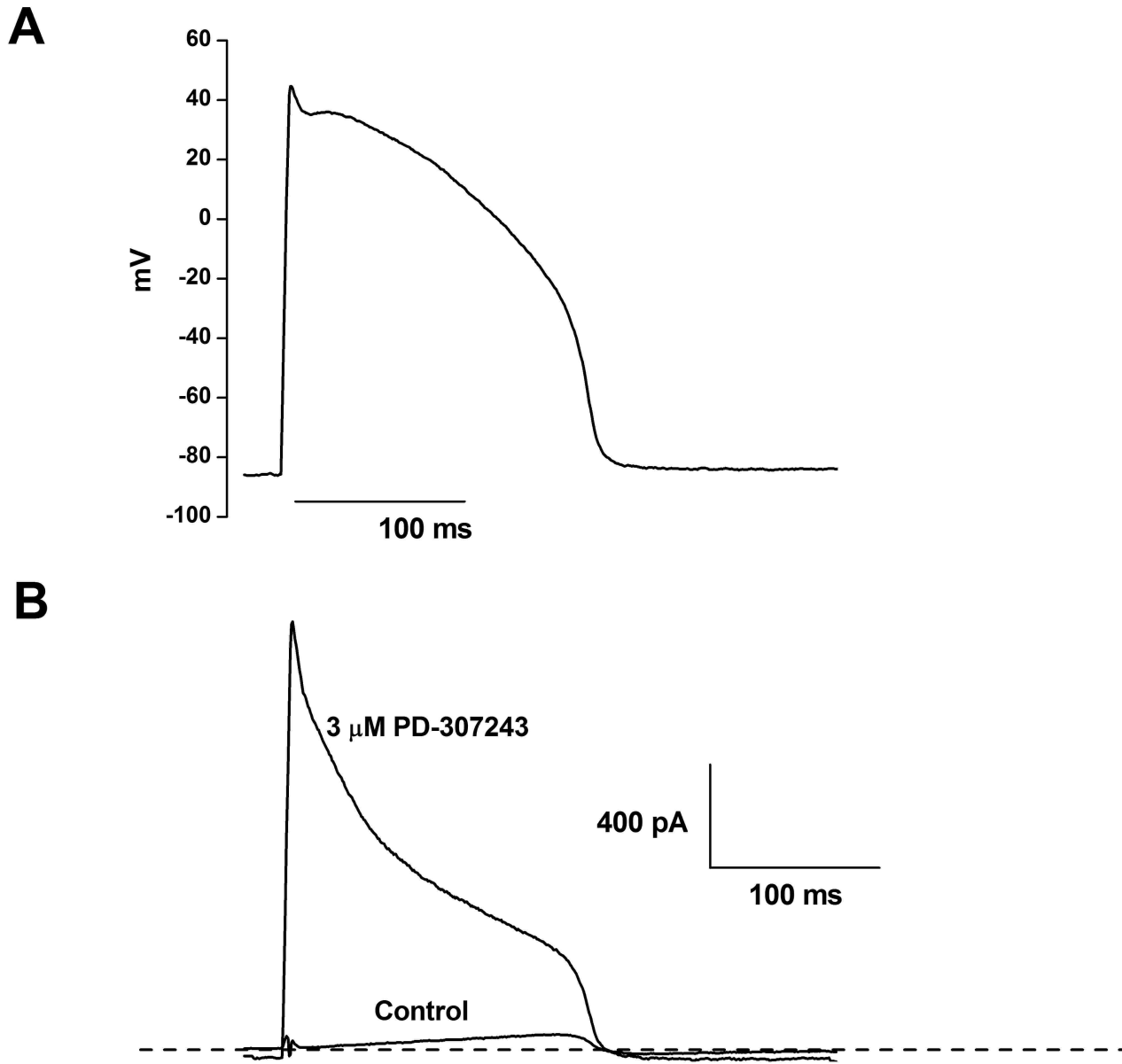


Figure 10

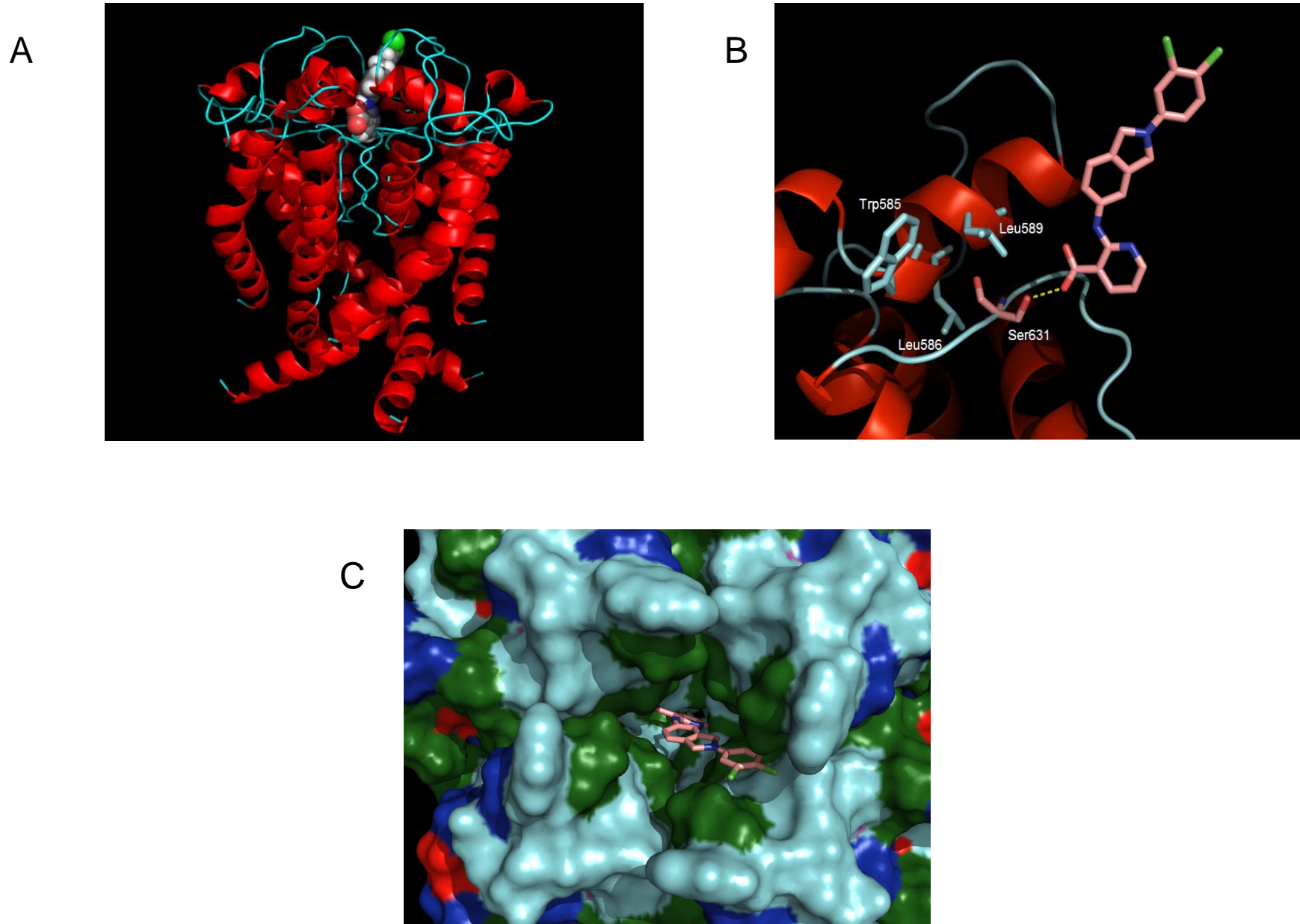


Figure 11